Mechanical Characterization of Micromachined Glass-Blown 3-D Spherical Shells

I.P. Prikhodko*, S.A. Zotov, A.A. Trusov, A.M. Shkel

MicroSystems Laboratory, Mechanical & Aerospace Engineering, University of California, Irvine, CA

ABSTRACT

This paper reports a non-contact experimental characterization of resonant modes in micromachined spherical shells fabricated by pressure and surface tension driven plastic deformation (glassblowing). For a glass-blown shell with 0.9 mm diameter and 10 μm average thickness, dynamically balanced 4- and 6-node vibratory modes were identified at 1.27 MHz and 1.44 MHz, respectively. Without any trimming or tuning of natural frequencies, the relative frequency mismatch $\Delta f/f$ for the 4- and 6-node vibratory modes was measured as 0.63% and 0.2%, respectively, on par with the state-of-the-art planar silicon MEMS. Glass-blown shells as resonant elements may enable new architectures of vibratory 3-D MEMS for high-g environments.

Keywords: 3-D MEMS, resonators, glassblowing, shells.

1 INTRODUCTION

Spherical shells are axisymmetric structures widely used in mechanical, civil, and aerospace engineering. The intrinsic property of axisymmetric shells is their superior resistance to distributed transverse loads. This quality in combination with structural symmetry and rigidity makes spherical shells attractive for use as mechanical vibratory elements in resonators, especially for high-g environments.

Until recently, micromachining of axisymmetric structures was limited to high temperature fusing of solid microspheres [1], [2], and isotropic etch of silicon spherical bowls [3]. The latter rely on photolithography and wet etch, leading to such fabrication imperfections as surface roughness, scalloping and footing of sidewalls. With the emergence of pressure and surface tension driven micromachining, or glassblowing [4], fabrication of smooth and symmetric spherical cells became feasible on a wafer level. This approach, initially developed for chip-scale atomic cells [5], relies on etching 0.8 mm deep and 0.5 mm wide cylindrical cavities into a silicon wafer, which is then anodically bonded to a 100 μm thick Corning Pyrex 7740 glass wafer. The wafer stack with sealed air pockets is then heated above the 850 °C softening point of Pyrex, leading to the formation of spherical shells, Fig. 1.

The current work investigates an intriguing possibility of using micro-scale glass-blown 3-D shells as mechanical vibratory elements, enabling new architectures of vibratory 3-D MEMS for signal processing, timing, and navigation applications. The paper reports experimental characterization of spatial vibrations and effects of fabrication imperfections on mechanical and dynamic properties of microshells.

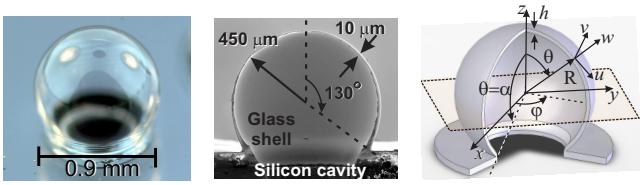

(a) Photograph. (b) Cross section. (c) Geometry.

Figure 1: Micromachined glass-blown spherical shell.

2 VIBRATIONS OF SHELLS

This section analyzes natural frequencies and mode shapes of glass-blown microshells considered as rigidly clamped, thin, elastic, spherical shells satisfying Kirchhoff-Love first approximation of shell theory, Fig. 1(c).

2.1 Equations and Assumptions

Based on Donnel-Mushtari-Vlasov assumptions [6], free vibrations of a spherical shell in terms of displacement components u, v, w, are governed by an 8^{th} order differential equation:

$$\begin{aligned} \Delta U + 2U &= -(1-\nu^2)(F_1+F_2), \\ \Delta V + 2V &= F_3, \\ \Delta\Delta w + 2\Delta w + c^2 w &= \frac{c^2 U}{1-\nu} + c^2 F_1 + 2(1-\nu^2), \end{aligned} \tag{1}$$

where Δ is Laplacian operator, $c^2 = 12(1-\nu^2)R^2/h^2$. Here,

$$U = \frac{\partial u}{\partial\theta} + u\cot\theta + \frac{1}{\sin\theta}\frac{\partial v}{\partial\varphi} - (1+\nu)w,$$

$$V = \frac{\partial v}{\partial\theta} + v\cot\theta - \frac{1}{\sin\theta}\frac{\partial u}{\partial\varphi}, \quad F_1 = -\frac{\rho R^2}{E}\frac{\partial^2 w}{\partial t^2},$$

$$F_2 = -\frac{\rho R^2}{E}\frac{\partial^2}{\partial t^2}\left[\frac{\partial U}{\partial\theta} + U\cot\theta + \frac{1}{\sin\theta}\frac{\partial V}{\partial\varphi}\right],$$

$$F_3 = \frac{2(1+\nu)\rho R^2}{E}\frac{\partial^2}{\partial t^2}\left[\frac{\partial V}{\partial\theta} + V\cot\theta - \frac{1}{\sin\theta}\frac{\partial U}{\partial\varphi}\right],$$

R and h are shell radius and thickness, E and ν are Young's modulus and Poisson's ratio, ρ is volumetric mass density.

Boundary conditions at $\theta = \alpha$ for a rigidly clamped shell

$$u = v = w = 0, \quad (\partial w/\partial\theta + u)/R = 0, \tag{2}$$

together with Eq. (1) define a well posed mathematical problem. The equation for natural frequencies [6]

$$f_m = \frac{1}{2\pi}\frac{\lambda_m}{R}\sqrt{\frac{E}{\rho(1-\nu^2)}}, \tag{3}$$

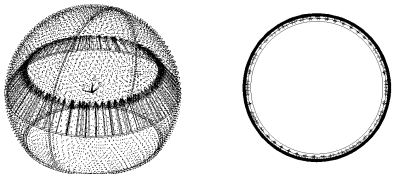

(a) Breathing mode, $m = 0$.

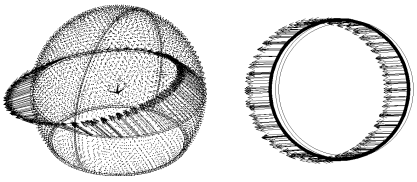

(b) Rocking mode, $m = 1$.

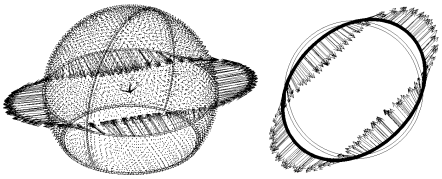

(c) Wineglass 4-node mode, $m = 2$.

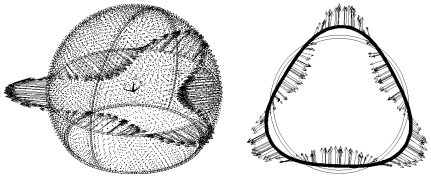

(d) Wineglass 6-node mode, $m = 3$.

Figure 2: Mode shapes of a clamped spherical shell, showing displacement distribution in 3-D and horizontal cross section.

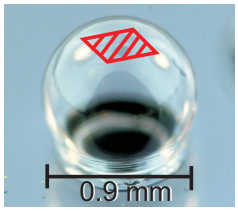

(a) Measured area $(5\ \mu\text{m})^2$

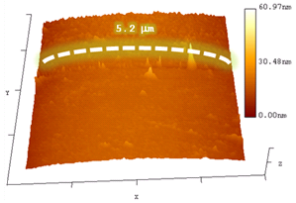

(b) Measured roughness 0.85 nm.

Figure 3: Surface roughness of glass shell measured with an atomic force microscope. Relative roughness is 1 ppm.

is obtained by applying Rayleigh-Ritz method and substituting displacements u, v, w into Eq. (1) in the form of $P_n^m(\cos\theta)\sin(m\varphi + \varphi_o)\cos(\omega t)$, where $P_n^m(\cos\theta)\sin(m\varphi)$ are spherical harmonics defining spatial mode shapes. The order m of a vibratory mode corresponds to the number of nodes (points of zero displacement) in a horizontal cross section of the shell.

The frequency parameter λ_m for given boundary conditions Eq. (2) and a mode order m depends on three parameters: geometry constants $h/R, \alpha$, and material ν. The dimensionless values λ_m were calculated for the typical geometry of micromachined glass-blown shell using $R = 0.45$ mm, $h = 10\ \mu$m, $\alpha = 130°$, $\nu = 0.2$ and converted to the natural frequencies using Eq. (3), which revealed spectrum of vibrations in MHz range, Table 1.

2.2 Mode Shapes

Finite element modal analysis was performed using MSC Patran to analyze mode shapes of glass-blown shells and compare with frequency values predicted theoretically, Fig. 2. The breathing mode, $m = 0$, Fig. 2(a) corresponds to the extension-compression of the sphere along the axis of symmetry. This motion results in a uniform distribution of displacement vectors, illustrated for the horizontal cross section. The rocking mode, $m = 1$, Fig. 2(b) involves side bending of a shell, which is seen in a horizontal cross section as an in-plane translation of every surface point except for the two nodes. The mode $m = 1$ is degenerate, and its second counterpart is spatially oriented $90°$ relative to the first.

Table 1: Comparison of resonant shell frequencies, kHz.

Mode	*Rocking*	*Breathing*	4-*node*	6-*node*
Theory	765	1329	1250	1493
FEM	799	1357	1291	1556
Experiment				
Shell no. 1	$692 \pm 0.7\%$	1186	$1271 \pm 0.3\%$	$1445 \pm 0.1\%$
Shell no. 2	$682 \pm 0.6\%$	1193	$1275 \pm 0.2\%$	$1434 \pm 0.1\%$

When shell vibrates in symmetric and dynamically balanced wineglass mode, $m = 2$ (or 3), shape is changing from circular to elliptical, Figs. 2(c) and 2(d). There are four (six) equally spaced polar zones on a shell for $m = 2$ (or 3). Consecutive zones move in opposite directions with $180°$ alternating phase. Degenerate counterparts for $m = 2$ (or 3) are spatially oriented $45°$ ($30°$) relative to each other.

The 4- and 6-node wineglass modes provide inherent rejection of common mode accelerations and are preferred for high g-force applications. The corresponding resonant frequencies obtained by FE modeling are within 3% of the frequency values predicted analytically, Table 1.

2.3 Effects of Fabrication Imperfections

Dynamically balanced wineglass modes used for resonant shell operation provide increased robustness to fabrication imperfections. Following analysis for a non-ideal ring resonator [7], variation of shell thickness $h(\varphi) = h + \Delta h\cos(2\varphi)$ in a horizontal cross section affect frequency f of two theoretically degenerate wineglass modes, leading to the relative mismatch $\Delta f/f = (3/4)(\Delta h/h)^2$. The same analysis for conventional planar mass-spring type resonators shows a strong linear sensitivity of the natural frequency f to the variation Δh in nominal beam width h governed by $\Delta f/f = (3/2)(\Delta h/h)$. The fabrication tolerance of 1% leads to frequency mismatch of 1.5% for mass-spring type resonators, and three orders of magnitude less (0.0075%) for a continuous resonant shell.

3 CHARACTERIZATION

This section reports experimental identification of mode shapes and mismatch in frequencies of fabricated prototypes.

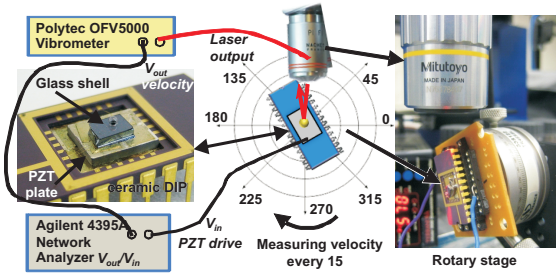

Figure 4: Schematic of the experimental testbed for non-contact characterization of glass-blown shells.

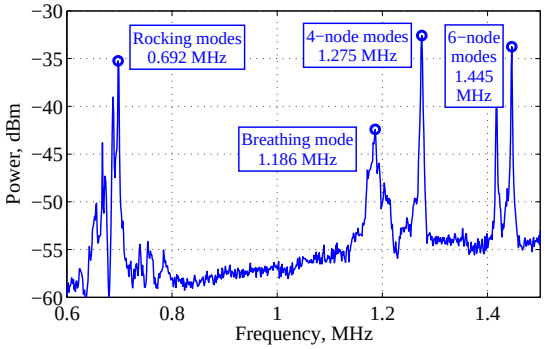

Figure 5: Frequency response of a glass-blown spherical shell, revealing resonant frequencies in the MHz range.

3.1 Surface Quality Metrology

Surface roughness is a performance limiting factor in mechanical resonant structures. The glassblowing process is expected to provide surface roughness improvement compared to the conventional fabrication processes based on etching. To investigate this hypothesis experimentally, several glass-blown shells were characterized using an Agilent Nano R2 Atomic Force Microscope (AFM). The initial average surface roughness of the Pyrex 7740 was measured as 0.48 nm over a $(5.2\ \mu\text{m})^2$ area. The average surface roughness after the fabrication was measured as 0.85 nm on the outer shell surface. This translates into the overall 1 ppm roughness relative to the 0.9 mm diameter of the shell, Fig. 3. Further reduction in shell roughness can be achieved by chemical polishing and controlling the level of impurities in the glassblowing furnace.

To compare the glassblowing technology with conventional surface micromachining, the same set of measurements was performed on a sidewall of a silicon resonator defined by DRIE using Unaxis Versaline VL-7339. Surface defects were measured as 17 nm over the same area, equivalent to 167 ppm roughness relative to the 100 μm beam thickness. This comparison demonstrates the potential of the glassblowing technology to produce high surface quality resonant microshells.

3.2 Identification of Mode Shapes

Inherent fabrication symmetry and measured low surface roughness suggest that glass-blown spheres can serve as high performance resonant elements. This section reports

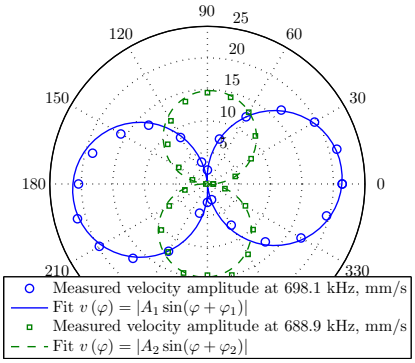

Figure 6: Measured velocity amplitude distribution along the equator of a spherical shell excited in rocking modes.

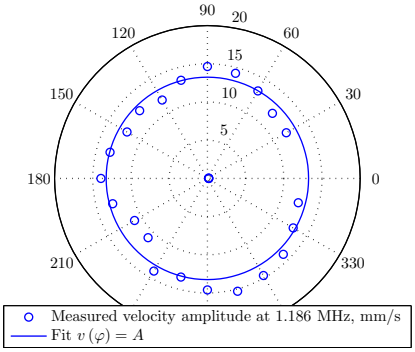

Figure 7: Measured velocity amplitude distribution along the equator of a spherical shell excited in a breathing mode.

structural properties of fabricated spheres measured using non-contact characterization methods facilitated by a Laser Doppler Vibrometer (LDV). For the experiment, a 3-D shell die was eutectically bonded to a piezoelectric (PZT) plate actuator and packaged in a ceramic DIP, Fig. 4. PZT enabled actuation over a wide spectrum range, thus exciting selected mode shapes. A Polytec OVF-5000 single-point LDV was used to directly measure velocities of surface points on the vibrating shell in real time.

For the experimental identification of resonant frequencies, the packaged glass-blown shell was mounted on a rotary stage in focus of the LDV, Fig. 4. By driving the PZT substrate with 5 V noise the returned power spectrum of vibrating shell, Fig. 5 revealed frequencies in the MHz range as predicted by the theory, Table 1. To identify mode shapes corresponding to each resonant peak, a scan was performed by rotating the packaged device with respect to the stationary LDV beam in 15° increments of longitude. The velocity amplitudes of the shell vibrating at 0.689 and 0.698 MHz were measured at 24 equally spaced points along the equator and plotted in polar coordinates, Fig. 6. The fit to surface harmonics $|A_i \sin(\varphi + \varphi_i)|$ revealed for each velocity map $i = 1, 2$ patterns with two nodes, suggesting that the shell was excited in rocking modes, $m = 1$. As expected from FEM, spatial orientation between the two degenerate modes is close to 90°. The vibratory mode at 1.186 MHz, Fig. 7 revealed a uniform velocity distribution suggesting that the shell is excited in a breathing mode, $m = 0$.

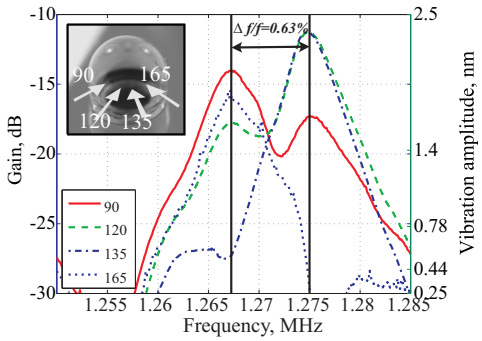

Figure 8: Measured frequency responses corresponding to the 4-node wineglass modes. Frequency mismatch is 0.63%.

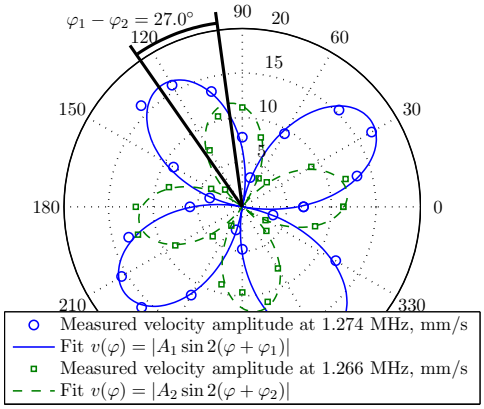

Figure 9: Measured velocity amplitude distribution along the equator of a spherical shell excited in 4-node modes.

For the next frequency range of 1.271 MHz $\pm 0.3\%$ modeling suggests two degenerate 4-node wineglass modes. To identify the frequency mismatch $\Delta f/f$, the frequency responses of the glass-blown shell were collected at several locations in the equatorial plane, revealing mismatch of only 0.63%, Fig. 8. The velocity maps corresponding to each resonant peak exhibit 4 nodal points, which is a characteristic property of a 4-node wineglass mode, Fig. 9. The relative spatial orientation between the two 4-node wineglass velocity patterns is defined by the principal axes of elasticity. The fit to the functions $|A_i \sin(2\varphi + \varphi_i)|$ revealed $\varphi_1 - \varphi_2 = 27°$ angle between the principal axes of elasticity, Fig. 9. The next pair of mechanical resonances was observed at 1.445 MHz $\pm 0.1\%$ corresponding to the 6-node modes of vibrations with measured $\Delta f/f = 0.2\%$, Fig. 10. Fitting the data to the mode shape $|A_i \sin(3\varphi + \varphi_i)|$ revealed a 7.5° angle between the principal axes of elasticity.

The mode shapes corresponding to each resonant peak, Fig. 5, were identified experimentally and summarized in Table 1, demonstrating a 7% agreement between the theoretical and measured frequencies.

4 CONCLUSIONS

We demonstrated the feasibility of using extremely smooth and symmetric microshells fabricated by wafer-level glassblowing as a mechanical resonant structures. The mode shapes and natural frequencies predicted analytically were

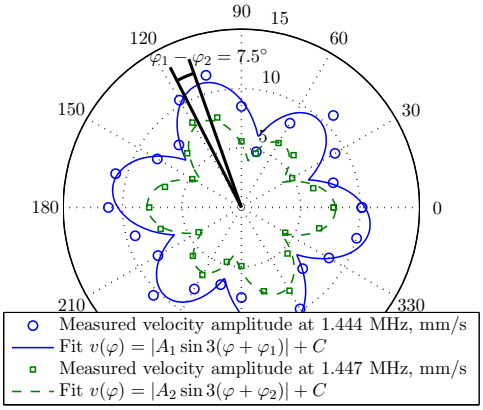

Figure 10: Measured velocity amplitude distribution along the equator of a spherical shell excited in 6-node modes.

confirmed experimentally with 7% agreement. Without any trimming or tuning of natural frequencies, the relative frequency mismatch $\Delta f/f$ for the 4- and 6-node vibratory modes was measured as 0.63% and 0.2%, respectively, on par with the state-of-the-art planar silicon MEMS, thus enabling fabrication of high precision devices with increased stability and resistance to high g-shock environments. The analysis presents a solid foundation for design of application-specific architectures of 3-D MEMS.

ACKNOWLEDGEMENTS

This work was supported by the National Science Foundation grant CMMI-0928999. Authors would like to thank the UCI INRF, MC2 and Carl Zeiss centers.

REFERENCES

[1] V.S. Ilchenko et al., "Microtorus: a High Finesse Microcavity with Whispering-Gallery Modes," Optics Letters, 26 (5), 256-258, 2001.

[2] D.H. Broaddus et al., "Silicon-waveguide-coupled high-Q chalcogenide microspheres," Optics Express, 17 (8), 5998-6003, 2009.

[3] K.D. Wise, M.G. Robinson, W. J. Hillegas, "Solid-state processes to produce hemispherical components for inertial fusion targets," Journal Vacuum Science and Technology, 18 (3), 1179-1182, 1981.

[4] E.J. Eklund, A.M. Shkel, "Glass Blowing on a Wafer Level," IEEE JMEMS, 16 (2), 232-239, 2007.

[5] E.J. Eklund, A.M. Shkel, S. Knappe, E. Donley, J. Kitching, "Glass-blown spherical microcells for chip-scale atomic devices," Sensors and Actuators, A: Physical, 143 (1), 175-180, 2008.

[6] V.Z. Vlasov, "General Theory of Shells and its Applications in Engineering," NASA TTF-99, 1964.

[7] S.A. Zotov, "Analysis of the effect of material anisotropic properties on the eigenfrequency of ring cavities of micromechanical gyroscopes," Semiconductors, 42 (13), 1557-1560, 2008.

CONTACT

* I.P. Prikhodko, tel: +1-949-824-6314; iprikhod@uci.edu.